Evidence for topological nonequilibrium in magnetic configurations

S. I. Vainshtein,[1] Z. Mikić,[2] R. Rosner,[1] and J. A. Linker[2]
[1]*Department of Astronomy and Astrophysics, University of Chicago, Chicago, Illinois 60637*
[2]*Science Applications International Corporation, San Diego, California 92121*
(Received 19 July 1999; revised manuscript received 13 January 2000)

We use direct numerical simulations to study the evolution, or relaxation, of magnetic configurations to an equilibrium state. We use the full single-fluid equations of motion for a magnetized, nonresistive, but viscous fluid; and a Lagrangian approach is used to obtain exact solutions for the magnetic field. As a result, the topology of the magnetic field remains unchanged, which makes it possible to study the case of topological nonequilibrium. We find two cases for which such nonequilibrium appears, indicating that these configurations may develop singular current sheets.

PACS number(s): 52.30.Bt, 47.65.+a, 52.65.Kj

I. INTRODUCTION

Formation of singularities, or current sheets, is one of the striking features of astrophysical as well as tokamak plasmas [1]. Such singularities are key to understanding active phenomena related to fast magnetic-field reconnection [2,3]. For example, fast dynamos rely on fast reconnection of magnetic-field lines [4,5]. Despite their importance, key issues related to current sheet formation are still not well understood. Supposing, e.g., that they are formed due to instabilities, one has to assume that fluid dynamical processes are able to slowly deform equilibrium magnetic-field configurations (and thereby build up regions of field gradients) without significant reconnection until a marginal state is reached. At this threshold, instability-driven reconnection would then lead to release of the stored free energy on the (observed) time scales thought to be too short to be consistent with, for example, Sweet-Parker reconnection [3,4]. However, it has been long recognized [6] that in the presence of reconnection, it is not obvious how one can attain (meta)stable configurations which store significant free energy. Furthermore, it is not clear why reconnection would not simply return the system to the marginal state, thus releasing only a small fraction of the available free energy.

In this paper, we explore one possible solution to these puzzles: We consider specific magnetic-field configurations which could arise from a slow evolution of (stable) quasiequilibria, and then examine their subsequent (unforced) evolution. Our aim is to show that there exist configurations that evolve initially on the slow rate, but that can reach a point at which spontaneous current sheet formation occurs. These configurations have been referred to as ''topological nonequilibria'' (TN) [2,7], and lead to situations in which the topology of the field is such that in a relaxed equilibrium state it inevitably contains discontinuities. TN results in spontaneous reconnection, because no external forces are involved; and in the cases we shall examine, the result is that extraction of all of the available free energy becomes possible.

Finally, we note that an important aspect of this problem relates to the fact that there is a direct correspondence between magnetostatic equilibria and steady Euler flows, as pointed out by Moffatt [8]; this problem is therefore closely connected to the possible formation of singularities in hydrodynamics; see also [9,10].

II. DESCRIPTION OF THE APPROACH

A. The idea of topological nonequilibrium

The main ideas of topological nonequilibrium (henceforth, TN) were formulated rigorously by Moffatt [8–10]. Consider an ideally conductive viscous (ICV) flow. We restrict ourselves to incompressible flows. Starting with initial magnetic field $\mathbf{B}(\mathbf{x},t=0)=\mathbf{B}_0(\mathbf{x})$ of arbitrary topology, one expects that such a configuration will relax to a static state, with zero velocity field, and nontrivial magnetic field $\mathbf{B}_E$. The latter configuration is then called ''topologically accessible'' because the field's topology does not change during this frozen-in evolution. If this relaxed equilibrium state contains discontinuities, then all of the states in the evolution are referred to as TN. It may be expected in a realistic situation, when small but finite resistivity η is taken into account, that these discontinuities evolve into finite-width current sheets, resulting in efficient reconnection and dissipation of the magnetic field. Unfortunately, there are only a few special cases for which it is possible to demonstrate that TN exists [11]. In this paper, we restrict ourselves to analysis of two-dimensional configurations, and study the evolution of two generic field configurations which can lead to TN.

Of course, in general, there is no reason that a given initial configuration is at equilibrium. However, one would normally expect that, after relaxation, such a configuration would evolve to attain a smooth equilibrium, and that the magnetic-field evolution subsequently stops. Some initial field topologies, however, cannot possibly relax to a smooth equilibrium, resulting in TN. It is obvious that use of the word ''nonequilibrium'' is not strictly correct, because in the final state the field *is* at equilibrium as long as the diffusivity vanishes exactly. However, in the spirit of maintaining an already existing tradition, we retain this terminology.

As a result of relaxation, the magnetic field will reach an equilibrium state. In two dimensions, $B_x=\partial_y A$, $B_y=-\partial_x A$, and the flux A obeys in equilibrium the equation

$$\nabla^2 A=-4\pi\frac{dP(A)}{dA}, \tag{1}$$

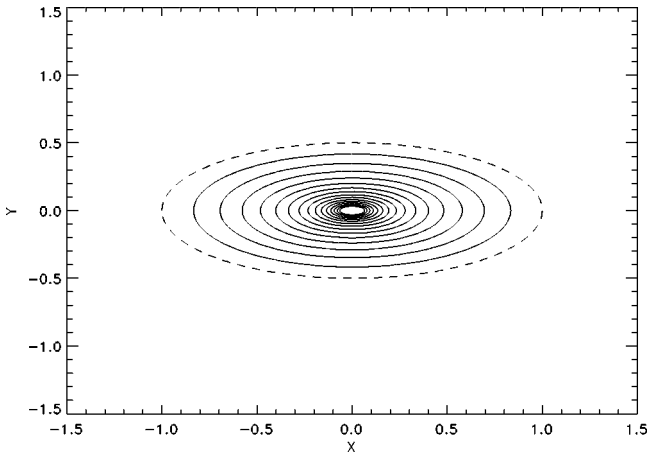

FIG. 1. Sketch of the type-*A* topology configuration: closed nested magnetic-field lines. The dashed line here, as in all the figures below, corresponds to a field line with vanishing magnetic-field strength.

where $P=p+B_z^2/(8\pi)$, $p=p(A)$, and $B_z=B_z(A)$; see, e.g., [12]. As an aside, we note that if the pressure p can be neglected, then this equilibrium is force-free; this may occur in specific applications such as in the solar corona. In addition, the total pressure P [Eq. (1)] ought to substantially exceed the transverse magnetic energy $B_x^2+B_y^2$ in order to justify the incompressibility assumption for the evolution to this equilibrium state.

Equation (1) is trivially satisfied in the one-dimensional case. To start with, suppose that A is a function of x only, corresponding to straight field lines parallel to the y axis. An initial arbitrary distribution is generally not at equilibrium. However, after relaxation, the field reaches the well-known equilibrium

$$\frac{B_y(x)^2}{8\pi}+P(x)=\text{const}, \tag{2}$$

automatically satisfying Eq. (1). The same is true for axisymmetric configurations, when $A=A(r)$, and the field consists of concentric circles.

Going to two dimensions complicates the problem considerably. Consider first a configuration with closed nested field lines, so that $A(x,y)$ has one maximum (minimum). The configuration is depicted in Fig. 1, and we will refer to it below as ''case *A*.'' Of course, the axisymmetric configuration is topologically accessible from this configuration, and therefore it can reach equilibrium. The question, however, is whether this equilibrium is unique.

If there exists a magnetostatic equilibrium with type-*A* field topology with essentially arbitrary field line geometry, e.g., with elliptic field lines, as in Fig. 1, then we would expect an arbitrary type-*A* configuration to relax to this equilibrium without dramatic changes in its geometry. However, suppose this equilibrium exists only in axisymmetric form, i.e., can only be realized with concentric (field line) circles; then, if this configuration were placed between magnetic ''walls'' (such as regions of strong magnetic fields in the solar corona, or solar wind), as in Fig. 2(a), we would expect the formation of discontinuities (because it would not be possible to evolve to the equilibrium state). Furthermore, if

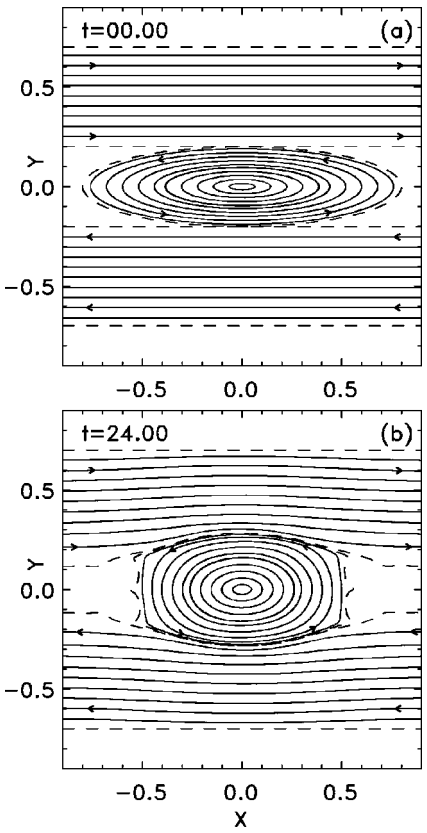

FIG. 2. Ellipse-shaped configuration placed between two horizontal magnetic walls; the initial configuration was generated by considering two families of (parametric) curves, i.e., straight lines and ellipses, and joining them as shown in panel (a). As a result of evolution of the configuration shown in panel (a), the field evolves such that it is pushed to the walls to form discontinuities, as shown in panel (b). Dashed lines correspond to $\mathbf{B}_\perp=\mathbf{0}$. Both panels present results of numerical simulations, but only selected field lines are depicted for illustrative purposes.

we allowed for nonvanishing diffusion, then such a configuration would not settle down until *all* magnetic lines are reconnected, and the bubble seen in Fig. 2 disappears entirely.

It is useful to expand slightly on the astrophysical relevance of this case. Our point is that ''case *A*'' shown in Fig. 2(a) can be regarded as an abstraction of a commonly expected field configuration in the solar atmosphere: Consider the emergence of a magnetic flux tube from the solar interior to the corona, where it enters a highly conducting medium already suffused by preexisting magnetic fields. If one abstracts such an emerging flux tube as a rising cylinder, then the expected field topology in planes perpendicular to the tube axis should be similar to case *A*: The nested closed field lines in such planes then represent the toroidal field component of the emerging flux tube; and the magnetic ''walls'' shown in Fig. 2(a) represent the projections in such planes of the magnetic fields of the surrounding magnetized coronal plasma.

The second type of field topology we consider below is what we call type *B*; this more complicated topology is a ''rosette structure'' [Fig. 3(a)], which has been investigated experimentally [13]. In terms of the flux function $A(x,y)$, this configuration consists of two maxima, e.g., two ''moun-

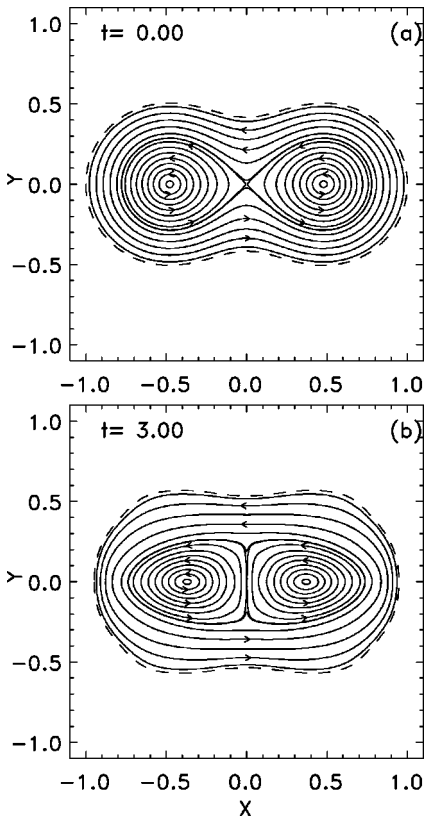

FIG. 3. Simulations for the (initially continuous) rosette structure, as depicted in panel (a). As a result of the relaxation, this configuration evolves into a field containing a discontinuity between the two magnetic islands, as shown in panel (b). The presence of the external zero line (dashed line) is vital for TN.

tains,'' surrounded by a pedestal, i.e., two magnetic islands surrounded by closed magnetic-field lines going around the two islands; the field vanishes outside the zero line. If the type-*B* topology cannot exist in smooth equilibrium, then a current sheet develops, resulting in efficient reconnection of field lines until all field lines of the islands are reconnected, and eventually only one island remains, of the topology of the type *A*. In contrast, if this kind of topology does exist in smooth equilibrium, then nothing dramatic would happen, and the configuration would relax to this equilibrium without any discontinuities. The astrophysical context in which this type of configuration may be created is similar to that just described above: consider the emergence of two adjacent twisted solar flux tubes into a nonmagnetized ambient corona; again, the field structure in a cross section perpendicular to the tube axes will appear as shown in Fig. 3(a). Thus, in both cases *A* and *B*, we are dealing with the generic case of bounded magnetic flux systems (i.e., systems of magnetic-field lines which lie within a finite bounding surface on which the field vanishes), which can be regarded as abstractions of, for example, isolated flux tubes emerging into the highly conductive solar corona.

Generally, finding TN states is far from trivial. To illustrate, let us return to the type-*A* topology. The axisymmetric equilibrium solution is *not* unique. For example, one can construct a solution to Eq. (1),

$$A(x,y)=\sin kx \sin ky,$$

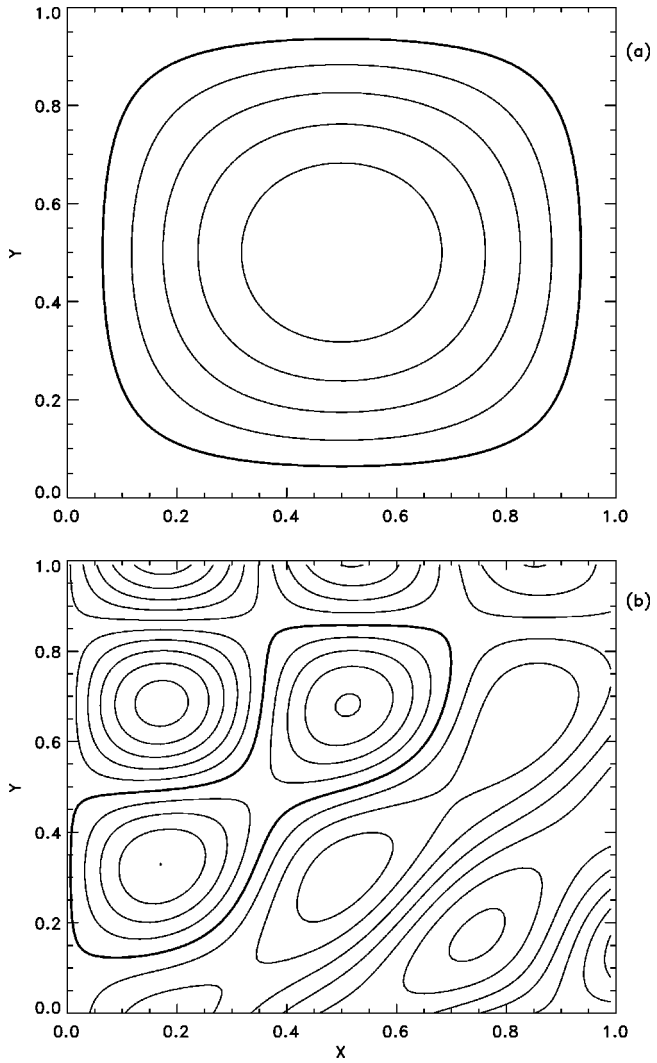

FIG. 4. Two examples of field configurations which share the field topology of the two cases (*A* and *B*) we are studying, which do not have any simple symmetries, but are nevertheless smooth equilibria. (a) Type *A* (marked by the thick line); (b) type *B* (rosette structure, marked by a thick line).

depicted in Fig. 4(a), which has the same topology of field lines as depicted in Fig. 1. This asymmetric field is at equilibrium, so that the general answer to the question of whether, say, elliptic configurations of the form shown in Fig. 1 can be at equilibrium, is affirmative. An analogous construction can be carried our for the topology of type *B*; in this case, the solution of Eq. (1) can be constructed as

$$A_z=\sum_n A_n e^{ik_x^{(n)}x+ik_y^{(n)}y},$$

where $(k_x^{(n)})^2+(k_y^{(n)})^2=\text{const}$ (see, e.g., [16,7]). This example is depicted in Fig. 4(b); the rosette structure shown is at equilibrium without any discontinuities.

The situation changes if a zero line (a line where $\mathbf{B}_\perp=0$, $\mathbf{B}_\perp=\{B_x,B_y\}$, and generally $B_z\neq 0$) is present, such as the dashed line shown in Fig. 1 for the type-*A*, and in Fig. 3 for the type-*B* field topology. The zero line possesses two remarkable properties. First, the magnetic field remains zero

on this line in the presence of ICV flow. Thus, if we write the ideal induction equation in the form

$$\frac{d\mathbf{B}}{dt}=(\mathbf{B}\cdot\nabla)\mathbf{v},$$

which in 2D reads

$$\frac{d\mathbf{B}_\perp}{dt}=(\mathbf{B}_\perp\cdot\nabla)\mathbf{v},\quad \frac{dB_z}{dt}=0, \tag{3}$$

it is easy to see that because the left-hand side describes transport of any fluid element (in particular, of the zero line) by the motion, and because the right-hand side corresponds to change of the field along the Lagrangian trajectory (and as the right-hand side vanishes on the zero line), this equation will preserve the property $\mathbf{B}_\perp=\mathbf{0}$ on the zero line.

Second, if the zero line has a constant (along the line) curvature, e.g., is a straight line or a circle, and if the field is also analytical, then the entire configuration will have the same geometry as the zero line. In other words, if the zero line is a straight line, then all other field lines are straight as well; alternatively, if the zero line is a circle, then the analytical equilibrium configuration consists of concentric circles. The proof is easily constructed by expanding $A(x,y)$ in the vicinity of the zero line [12]. Note, however, that the constant curvature zero line is a special case (although it can be regarded as a representation of the emergence of magnetic flux on, for example, the solar surface, in which geometrically symmetric flux bundles straddle the separating ''neutral line''); in general, the zero line is arbitrary in shape, as shown in Figs. 1–3. Nevertheless, we may conjecture that the zero line imposes a severe constraint on the geometry: That is, we conjecture that the existence of this line results in unique (smooth) solutions of Eq. (1) in the form of magnetic-field lines with constant curvature [12].

One of the considerations in favor of this conjecture is as follows. Without loss of generality, $A\equiv 0$ outside the configuration, and thus $A=0$ on the boundary (whose shape is as yet unspecified), corresponding to the Dirichlet problem for Eq. (1). On the other hand, because $B_x=B_y=0$ on the same boundary, we have $\partial_n A=0$, corresponding to a Neumann problem. The problem is thus overconstrained; and one would expect this to lead to degeneracy of the solution. That is, these specific boundary conditions are expected to restrict the shape of the boundary itself, and thus in turn to restrict the topology of possible equilibria. Although the boundary conditions are specified, and the problem is thus rigorously formulated, the above statement regarding the overconstrained nature of our problem nevertheless has not been shown to be useful in constructing a formal mathematical proof concerning the geometry of the configuration in the presence of a zero line. Formally, it is easier to discard the TN for a given topology by direct construction of a solution with needed properties. Generally, it is not clear at all how to construct a formal proof that the only solution of Eq. (1) with boundary condition $\mathbf{B}_\perp=0$ for the type-*A* topology is unique, and axisymmetric, thus defining the shape of the boundary itself. It is even less clear how to prove that there is no smooth solution for the type-*B* topology, assuming that this statement is true.

Note that one can simply produce artificial discontinuities, but these are irrelevant to our discussion. To illustrate, suppose that we place superconductive walls at the locations of the thick lines in both panels of Fig. 4. In that case, the configurations will be at equilibrium (for both type-*A* and -*B* topologies), and the field will be smooth everywhere except at the boundaries (where the field jumps from a finite value just outside the walls to zero at the walls in order to meet the boundary condition of zero field within the superconducting walls). This type of discontinuity is irrelevant to the astrophysical problem we are aiming at, and we therefore do not discuss it any further.

Thus, the ideally conductive flow does allow magnetic-field discontinuities and discontinuities in current distributions. However, studying the current sheet formation, we should not allow them to be present at the very beginning, that is, the initial configuration should not contain magnetic discontinuities. This kind of configuration, with zero line, i.e., localized in space, and with nontrivial symmetry, can be easily constructed analytically. For example,

$$A(x,y)=(\sin k_x x\sin k_y y)^2, \tag{4}$$

for $0\leqslant x\leqslant \pi/k_x$, $0\leqslant y\leqslant \pi/k_y$, and $A(x,y)\equiv 0$ outside this domain. Clearly, $A(x,y)=0$ and $B_x=B_y=0$ on the boundary, although the current experiences a jump. In order to avoid this, consider

$$A(x,y)=(\sin k_x x\sin k_y y)^3, \tag{5}$$

then the current also goes to zero on the boundary. However, as the jump of the current is allowed even at the beginning of the process, the configuration (4) is satisfactory for our needs. The topology of both Eqs. (4) and (5) coincides with the *A* type, depicted in Fig. 1 or Fig. 4(a). One can apply continuous deformations in the plane to this potential $A(x,y)$, and still retain the desired property that $\mathbf{B}=0$ on the boundary [see Eq. (3)]. It is easy to check that neither Eq. (4) nor Eq. (5) satisfies the equilibrium condition (1). The nontrivial question is, however, if any if these transformations (except the axisymmetric one) can be at equilibrium.

B. Description of the solution method

One of the powerful ways to study the formation of current sheets is via numerical simulation. However, in numerical simulations the Lundquist number, $S=c_A L/\eta$ (c_A the Alfvén speed and L the characteristic length), which is critical for this problem, is far below that corresponding to values encountered in natural systems, viz., under astrophysical conditions [3]. When S is not sufficiently large, the separation between typical reconnection times and typical fluid dynamical times may not be large; it is therefore difficult to interpret realistic resistive calculations in the context of a problem in which current sheet formation is to occur without topological changes. On the other hand, numerical schemes which attempt to circumvent this problem by solving the ideal MHD equations suffer from the difficulty that such schemes may be subject to numerical instability, so that it becomes difficult to distinguish between numerical artifact and physically correct current sheet formation. When discontinuities in the magnetic field appear, traditional numerical

MHD codes tend to either break down or to introduce a small amount of resistivity to broaden the current sheets (so that, for example, their width is larger than a mesh cell). In certain situations, the symmetry of the problem can be exploited to study the approach to the ideal solution, i.e., $\eta \to 0$, see, e.g., [14]. However, typical simulations actually add some amount of numerical resistivity, as in [10], so that numerical solutions of the ideal induction equation correspond to solutions of that equation with an added effective diffusivity. In studies of reconnection it is known that the specification of boundary conditions on the magnetic field and velocity (which specify the rate at which magnetic field and plasma is brought into the reconnection layer) may affect the rate of reconnection. In our simulations, we study spontaneous formation of singularities by isolating the flux system from the boundaries. We surround our flux bundle by a (transverse) field-free region, and we place the boundaries far away from the bundle, thereby minimizing the effect of the boundary conditions on the formation of the current sheets.

We address this issue as a relaxation problem in the framework of ICV flows. Our approach involves a direct numerical simulation of ICV flows, i.e., solving the set of equations (3) and the momentum equation,

$$\frac{d\mathbf{v}}{dt} = \frac{\partial \mathbf{v}}{\partial t} + (\mathbf{v}\cdot\boldsymbol{\nabla})\mathbf{v} = -\frac{1}{\rho}\boldsymbol{\nabla} p + \frac{1}{4\pi\rho}\{\boldsymbol{\nabla}\times\mathbf{B}\}\times\mathbf{B} + \nu\boldsymbol{\nabla}^2\mathbf{v}, \tag{6}$$

with $\boldsymbol{\nabla}\cdot\mathbf{v}=\mathbf{0}$ [15]. We use a Lagrangian approach to solve the induction equation (3), as in [17,5]. More specifically, the magnetic field inside the region of interest is represented by a large number of field lines; the evolution of the field lines is then followed using the exact Lundquist solution, i.e., knowing the initial strength of the magnetic field on a fluid element connecting two nearby points on a field line, the final strength is proportional to the length of the segment, as it is stretched by the motions. We assume for all cases that the magnetic field vanishes on the outermost field line (the dashed curves shown in the figures). The number of field lines which fill the domain is chosen so that the subsequent field evolution can be followed without leaving gaps in the final state, i.e., we determine the number of initial field lines by fixing the spatial resolution of the final state; we discuss this point further immediately below. As an important aside, we note that the initial magnetic field is smooth, implying that the current system, $\mathbf{j}(x,y)$, which is defined by Ampere's law

$$\boldsymbol{\nabla}\times\mathbf{B} = \frac{4\pi}{c}\mathbf{j},$$

is smooth as well, i.e., there are no current sheets initially.

The momentum equation (6), in contrast, is solved using standard finite difference techniques, with finite viscosity. However, the requirement of coupling the magnetic-field evolution to the momentum equation does lead to a complication for computing the Lorentz force. The key issue is that the momentum equation requires the Lorentz force to be evaluated on a homogeneous spatial grid, while the magnetic-field evolution is given in Lagrangian space. We resolve this issue by (quadratically) interpolating the Lorentz force at each time step onto the homogeneous grid used by the momentum equation (6); similarly, we use quadratic interpolation from the momentum equation mesh to evaluate the velocity field on the Lagrangian mesh. In order to minimize interpolation errors, we fix the number of field lines such that every Eulerian grid domain is pierced by at least a few field lines throughout the calculation. Note here that interpolation errors do lead to inaccuracies in the solution of the flow and magnetic fields, but by construction cannot lead to changes in the magnetic-field topology. Note also that we have checked for convergence of the solutions as the spatial resolution of our calculation is increased; our conclusion is that the results presented here do not depend on grid resolution. Our solution corresponds to the limit $\eta \to 0$, in the sense that the topology is strictly conserved, but with finite viscosity; thus, the computational scheme we use forces the relaxation to be due solely to viscous damping, and as a consequence, the field relaxes to an equilibrium state. Our approach has the dual virtues that the boundary conditions for the magnetic field do not need to be specified, and that the field topology is preserved; it is therefore appropriate for the study of TN.

If the viscosity is large, then Eqs. (3)–(6) describe monotonic relaxation to equilibrium. We can estimate the relaxation time as follows: from Eq. (6) we find that $v \sim c_A^2 L/\nu = c_A S_\nu$, where $S_\nu = c_A L/\nu$. This viscous regime is realized if $S_\nu \ll 1$. The relaxation time is then $t_\nu \sim L/v = \tau_A/S_\nu$, with $\tau_A = L/c_A$. In the opposite limiting case, $S_\nu \gg 1$, the system undergoes (strong) Alfvén oscillations ($v \approx c_A$), with a period τ_A, decaying on a viscous time $t_\nu \sim L^2/\nu = \tau_A S_\nu$. These two cases can be jointly described by an interpolation formula,

$$t_\nu = \tau_A(S_\nu + 1/S_\nu),$$

from which it follows that the relaxation time is large for both limiting cases (in terms of τ_A). Thus, optimal relaxation to equilibrium occurs for $S_\nu \sim O(1)$; in the simulations, we used the value $S_\nu = 5$. It is important that S_ν not be too large: An important constraint on the value of S_ν is that the simulations remain stable. This constraint is not met if S_ν is too large; because the two dynamical equations are solved in different coordinates [Eq. (3) in Lagrangian, and Eq. (6) in Eulerian coordinates], errors arise from the interpolation from one coordinate system to the other, and therefore the calculations make sense only if these errors are damped sufficiently by viscosity.

III. DESCRIPTION OF THE RESULTS

We conducted two series of numerical experiments for case *A*. In the first series, we consider the relaxation of this type of topology without any external field, as depicted in Fig. 1. We explored different initial shapes of the field lines, including ellipselike, diamondlike, and other similar configurations. In addition, for a fixed shape, we explored different distributions of the flux function $A(x,y)$, i.e., different functional dependences $A(s)$, where s labels the field lines. The results are always the same: the field ends up in an axially symmetric state, provided the field vanishes on the outermost field line.

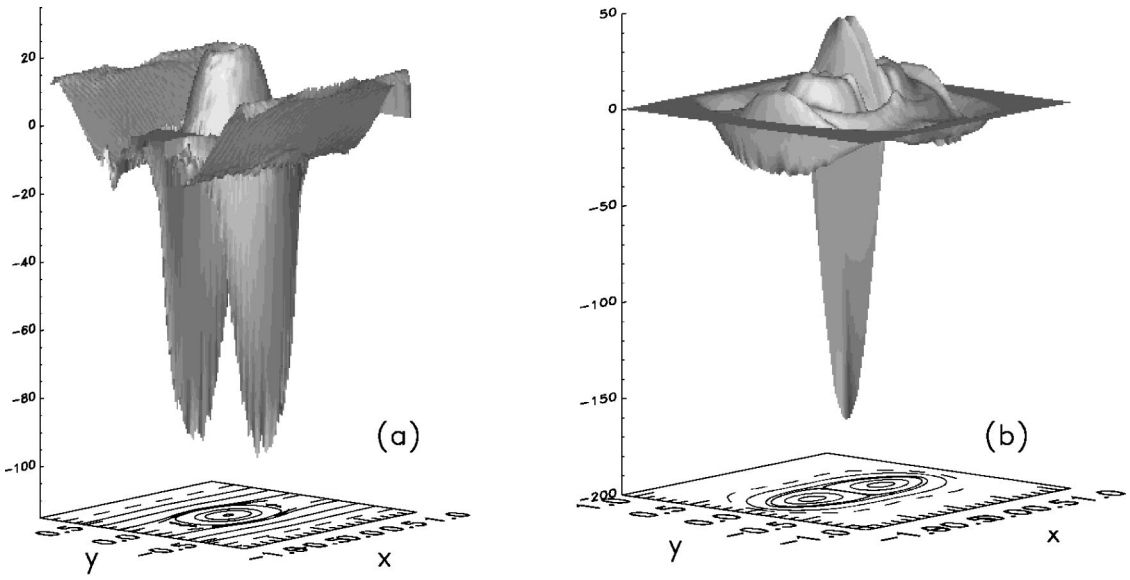

FIG. 5. Profiles of the z current corresponding to (a) the topology of Fig. 2(b), and to (b) Fig. 3(b) [the field line configurations of Figs. 2(b) and 3(b) are reproduced at the bottoms of (a) and (b), respectively]. The current sheets are represented by negative currents. Due to the presence of an external zero line, the total current is zero, and therefore strong and peaked negative current is compensated by a spatially distributed positive current. Note that in panel (a), the current corresponding to the external field of the magnetic walls changes sign, because each wall contains two zero lines.

In another set of experiments, this same configuration (case A) is placed between magnetic walls, as in Fig. 2(a); in this case, the system always evolves to create discontinuities, as in Fig. 2(b), where the field lines are taken from one of our simulation runs. We see that as the ''bubble'' evolves, it attempts to become axisymmetric, but as it does so, two discontinuities begin to form, as depicted in Fig. 2(b), see also Fig. 5(a). It is interesting to note that, for some initial conditions, a *current point* is formed, rather than a current sheet (or a line in two dimensions), suggesting that finite conductivity could presumably result in fast reconnection; that is, according to the Sweet-Parker mechanism (see, e.g., [4]), the reconnection rate $v_d \sim 1/\ell$, where ℓ is the length of the current sheet, so that a short current sheet speeds up the reconnection. (In the classical Sweet-Parker mechanism, $\ell = L$, and $v_d = c_A / S^{1/2}$.)

It is crucial to note here that the evolution we just described is not forced by the walls; thus, the field and fluid near the walls (i.e., on the wall side of the zero lines) have the equilibrium property (2). To see this, note that on the zero line, the total pressure is continuous. Thus, we could replace the initial elliptical field configuration (the ''bubble'') lying between the two zero lines with a field-free region whose gas pressure exactly balances the total pressure on the wall side of the zero lines. The resulting configuration is clearly in equilibrium, and makes clear that the walls do not push the bubble, i.e., that the evolution of the bubble is entirely driven by the fact that it is not in equilibrium. Thus, it is as the bubble tries to become axisymmetric, and pushes back the walls, that the two discontinuities are formed. In principle, if the bubble could reach equilibrium with ellipse-shaped field lines as in Fig. 2(a), then it would not even interact with the walls, and the equilibrium of the whole configuration would be smooth. The field evolution to TN here described, i.e., evolution from an initially smooth state to a state containing a singularity, is therefore an intrinsic property of the initially smooth state, rather than being forced by external means.

Consider now the type-B configurations. We again conducted two series of experiments. In the first series of numerical experiments, we studied different kinds of initial states, with different initial field line shapes and with different distributions $A(s)$; in all cases, we again required that the outermost line must be a zero line, as shown in Fig. 3. We found for the type-B configuration that a field discontinuity always appeared, as in Fig. 3(b) (which is taken from one of our simulations), no matter what the initial distribution of A, or what kind of analytical representation of the initial field lines we used.

In the second set of experiments, we simulated the evolution of a magnetic field with a different number of field lines. The issue is as follows: The magnetic-field gradient at $x = 0$ increases during the evolution, so that the current, $\nabla \times \mathbf{B}$, approaches a δ function (Fig. 5). It is not possible to observe this tangential discontinuity because in the simulations the field is described via a finite (albeit a very large) number of field lines (recall [18]). Our hypothesis is that in the limit of an infinite number of field lines $N \to \infty$, the current at $x = 0$ tends to infinity; in order to test this hypothesis, we increased the number N (recall [19]) in a succession of simulations that were otherwise identical. According to our hypothesis, we expected the current to grow roughly as $1/\Delta$, where Δ is the closest distance between the X point and the nearest field line; the experiments confirmed this expectation.

IV. CONCLUSION

The fundamental result emerging from our simulations is that the vanishing magnetic field on the outermost field line imposes strict constraints on the geometry of equilibrium: The type-A topology can be at equilibrium only if it is axi-

symmetric; and therefore, if constrained by external walls, it is at TN. Similarly, the type-*B* rosette structure develops discontinuities, but only in the presence of an external zero line. The presence of zero lines is thus an important aspect of topological nonequilibria.

Finally, we comment briefly on the applicability of these results to astrophysical situations. Observations of the solar atmosphere [20] commonly show topologically unconnected magnetic flux systems which are seen to interact (viz., emerging flux loops). In such circumstances, in which one expects to encounter small but finite resistivity, these flux systems are initially unlinked, but as they are pushed together (and begin to reconnect), flux linkage is expected to occur and to lead to a field topology analogous to that depicted in Fig. 2, or to the generic type-*B* configuration discussed here. The magnetic flux surrounding these two islands would be initially weak, and the current sheet which is formed is therefore expected to be weak. However, during the course of reconnection, more flux will be pushed outside the two islands, thus accelerating the process of reconnection. This process may therefore be self-accelerating, resulting in final (spontaneous) reconnection; preliminary numerical simulations of a resistive case of this sort suggest that the reconnection rate v_d scales as c_A/S^{α}, where α is a small power, $\alpha \sim O(0.1)$ [21]. If confirmed, it would imply that the reconnection is fast enough to satisfy the observed (solar) constraints on reconnection times. (Recall that while the Sweet-Parker reconnection time for typical parameters corresponding to the solar corona is about three years, the time corresponding to $v_d = c_A/S^{0.1}$ is only 30 min, which is comparable to the energy release time scale for large solar flares, related to the so-called ''long-enduring'' events [3].) Therefore, the two topologies depicted in Figs. 2 and 3 may be regarded as generic examples of ''fast'' reconnection and activity in magnetically active astrophysical systems.

ACKNOWLEDGMENTS

We have benefited considerably from comments by, and discussions with, H.K. Moffatt, E.N. Parker, and T. Emonet. This work has been supported by the NASA Space Physics Theory Program at the University of Chicago (R.R., S.I.V.) and, in part, by NSF Grant No. ATM-9320575, and NASA Contracts No. NAS5-96081 and No. NASW-5017 to SAIC (Z.M. and J.A.L.).

[1] M.N. Rosenbluth, R.Y. Dagazian, and P.H. Rutherford, Phys. Fluids **16**, 1894 (1973); M.N. Rosenbluth and M.N. Bussac, Nucl. Fusion **19**, 489 (1979).

[2] E. N. Parker, *Spontaneous Current Sheets in Magnetic Fields* (Oxford, New York, 1994).

[3] L. Golub and J.M. Pasachoff, *The Solar Corona* (Oxford University Press, Oxford, 1997).

[4] E. R. Priest, *Solar Magnetohydrodynamics* (D. Reidel, Dordrecht, Holland, 1981).

[5] S.I. Vainshtein, R.Z. Sagdeev, and R. Rosner, Phys. Rev. E **56**, 1605 (1997); S.I. Vainshtein, Phys. Rev. Lett. **80**, 4879 (1998).

[6] A.A. Galeev, Space Sci. Rev. **23**, 411 (1979).

[7] E.N. Parker, Astrophys. J. **174**, 499 (1972); *Cosmical Magnetic Fields* (Clarendon, Oxford, 1979).

[8] H.K. Moffatt, J. Fluid Mech. **159**, 359 (1985).

[9] H.K. Moffatt, J. Fluid Mech. **166**, 359 (1986); in *Turbulence and Nonlinear Dynamics in MHD Flows*, edited by M. Meneguzzi, A. Pouquet, and P. L. Sulem (Elsevier Science Publishers B. V., Amsterdam, 1989).

[10] K. Bajer and H.K. Moffatt, J. Fluid Mech. **212**, 337 (1990); D. Linardatos, *ibid.* **246**, 569 (1993); A.Y.K. Chui and H.K. Moffatt, Proc. R. Soc. London, Ser. A **451**, 609 (1995); A.Y.K. Chui and H.K. Moffatt, J. Plasma Phys. **56**, 677 (1996).

[11] B.B. Kadomtsev, Plasma Phys. **1**, 710 (1975); S.I. Vainshtein, Magn. Gidrodin. **3**, 269 (1988).

[12] S.I. Vainshtein, Zh. Éksp. Teor. Fiz. **86**, 451 (1984) [Sov. Phys. JETP **59**, 262 (1984)]; S.I. Vainshtein and E.N. Parker, Astrophys. J. **304**, 821 (1986); S. I. Vainshtein, A.M. Bykov, and I.N. Toptygin, *Turbulence, Current Sheets and Shocks in Cosmic Plasma* (Gordon & Breach, Amsterdam, 1993).

[13] M. Yamada, H. Ji, S. Hsu, T. Carter, R. Kulsrud, Y. Ono, and F. Perkins, Phys. Rev. Lett. **78**, 3117 (1997).

[14] Z. Mikić and J.A. Linker, Astrophys. J. **430**, 898 (1994).

[15] Note that Moffatt and collaborators [10] treat the relaxation problem in quasistatic porous media, so that their momentum equation differs from ours.

[16] M.B. Isichenko, Rev. Mod. Phys. **64**, 961 (1992); M.B. Isichenko and A.V. Gruzinov, Phys. Plasmas **1**, 1802 (1994).

[17] S.I. Vainshtein, R.Z. Sagdeev, R. Rosner, and E.-J. Kim, Phys. Rev. E **53**, 4729 (1996).

[18] In our approach, it is necessary for each Eulerian cell to contain at least several field lines. Therefore, as we increase the spatial resolution of the Eulerian grid, we need to correspondingly increase the number of field lines used for the Lagrangian calculation.

[19] In order to resolve the same field with increased *N* adequately, we have to increase the number of Eulerian cells; see [18].

[20] K. Shibata, N. Nitta, R. Matsumoto, T. Tajima, T. Yokoyama, T. Hirayama, and H. Hudson, in *X-ray Solar Physics from Yohkoh*, edited by Y. Uchida, T. Watanabe, K. Shibata, and H. Hudson (Universal Academic Press, Tokyo, 1993), pp. 29–32.

[21] S.I. Vainshtein, Z. Mikić, and J.A. Linker (unpublished). The relatively simple geometry of the configuration makes it possible to study the scaling of the reconnection rate with two decades of scaling in *S*. Presumably, the reconnection rate substantially exceeds the Sweet-Parker rate because the current sheet is relatively short. Low rates of reconnection observed in coalescing magnetic islands, see, e.g., C. Marliani and H.R. Strauss, Phys. Plasmas **6**, 495 (1999), may be attributed to the fact that the configuration is not at topological nonequilibrium, because there is no outermost zero line in the problem, so that the current sheet is instead formed due to instability.